

# Charge disproportionation in $R\text{NiO}_3$ perovskites ( $R$ =rare earth) from high-resolution x-ray absorption spectroscopy

M. Medarde,<sup>1</sup> C. Dallera,<sup>2</sup> M. Grioni,<sup>3</sup> B. Delley,<sup>4</sup> F. Vernay,<sup>4,\*</sup> J. Mesot,<sup>5</sup> M. Sikora,<sup>6,†</sup> J. A. Alonso,<sup>7</sup> and M. J. Martínez-Lope<sup>7</sup>

<sup>1</sup>Laboratory for Developments and Methods, Paul Scherrer Institut, 5232 Villigen PSI, Switzerland

<sup>2</sup>INFN, Dipartimento di Fisica, Politecnico di Milano, p. Leonardo da Vinci 32, 20133 Milano, Italy

<sup>3</sup>Institut de Physique de la Matière Condensée, Ecole Polytechnique Fédérale, 1015 Lausanne, Switzerland

<sup>4</sup>Condensed Matter Theory Group, Paul Scherrer Institut, 5232 Villigen PSI, Switzerland

<sup>5</sup>Paul Scherrer Institut, ETH Zürich and EPF Lausanne, 5232 Villigen PSI, Switzerland

<sup>6</sup>European Synchrotron Radiation Facility, 6 rue Jules Horowitz, BP 220, 38043 Grenoble Cedex, France

<sup>7</sup>Instituto de Ciencia de Materiales de Madrid, CSIC, Cantoblanco, 28049 Madrid, Spain

(Received 29 October 2009; published 4 December 2009)

High-resolution x-ray absorption measurements reveal a rare-earth-dependent splitting of the Ni  $K$  edge in the insulating, charge-disproportionated state of the whole  $R\text{NiO}_3$  perovskite family. The splitting is five times larger for  $\text{LuNiO}_3$  [2.5(1) eV] than for  $\text{PrNiO}_3$  [0.5(3) eV], suggesting that the charge transfer between  $\text{Ni}^{3+\delta}$  and  $\text{Ni}^{3-\delta}$  decreases by approaching the itinerant limit and is larger for the heavier lanthanides than suggested in previous studies. The spectroscopic signature of the two Ni sites remains visible above the metal-insulator transition, in agreement with the persistence of dynamic  $\text{Ni}^{3+\delta}/\text{Ni}^{3-\delta}$  charge fluctuations in the metallic phase. This last result generalizes the occurrence of charge disproportionation as alternative to Jahn-Teller distortions to the dynamic regime, giving further support to recent theoretical work [I. I. Mazin, D. I. Khomskii, R. Lengsdorf, J. A. Alonso, W. G. Marshall, R. M. Ibberson, A. Podlesnyak, M. J. Martínez-Lope, and M. M. Abd-Elmeguid, Phys. Rev. Lett. **98**, 176406 (2007)].

DOI: [10.1103/PhysRevB.80.245105](https://doi.org/10.1103/PhysRevB.80.245105)

PACS number(s): 71.28.+d, 71.30.+h, 71.45.Lr, 78.70.Dm

## I. INTRODUCTION

The crossover from localized to itinerant behavior in strongly correlated electron systems is a fundamental problem of solid-state physics.  $R\text{NiO}_3$  perovskites ( $R$ =rare earth) are well suited to an investigation of this region because, in contrast to most oxide systems, a complete evolution from itinerant to localized behavior can be achieved without doping. With the exception of metallic  $\text{LaNiO}_3$ , all members of the series display metal-to-insulator (MI) transitions at temperatures  $T_{\text{MI}}$  increasing with the decreasing size of the  $R$  ion (i.e., the bandwidth  $W$ ).<sup>1</sup> The gap opening is associated with a partial charge disproportionation (CD) of the type  $2\text{Ni}^{3+} \rightarrow \text{Ni}^{3+\delta} + \text{Ni}^{3-\delta}$ ,<sup>2</sup> where the two Ni sites alternate along the three pseudocubic perovskite axes forming a rock salt-like three-dimensional array. This scenario, initially developed for the heavy lanthanides, received further support from a number of experimental techniques<sup>3-5</sup> but it could only be generalized to the whole  $R\text{NiO}_3$  family after the recent observation of long-range  $\text{Ni}^{3+\delta}/\text{Ni}^{3-\delta}$  charge order in the low-temperature insulating phase of  $\text{PrNiO}_3$ .<sup>6</sup>

CD is often encountered in compounds containing broadband  $6s^1$  ions such as  $\text{Bi}^{4+}$ ,  $\text{Pb}^{3+}$ , or  $\text{Tl}^{2+}$  due to their strong tendency toward  $6s^0 + 6s^2$  closed shell configurations.<sup>7</sup> It is more surprising to observe it in highly correlated  $3d$  oxides where Coulomb repulsion usually prevents charge transfer between metallic sites. In the particular case of  $e_g^1$  systems, the occurrence of the  $2e_g^1 \rightarrow e_g^0 + e_g^2$  process has been interpreted as alternative to Jahn-Teller (JT) distortions.<sup>8</sup> First-principle band-structure calculations suggest that the relevant parameter for the choice of the stabilization mechanism is the ratio of the on-site Coulomb energy  $U$  and the electronic

bandwidth  $W$ . For insulators such as  $\text{LaMnO}_3$ ,  $U/W \gg 1$  and JT distortions are usually preferred. In itinerant systems such as  $\text{LaNiO}_3$ ,  $U/W \ll 1$ , the kinetic-energy term dominates and JT distortions are suppressed. In the intermediate regime with  $U/W \sim 1$ , the Hund's intra-atomic exchange  $J_H$  may overcome the effective Coulomb repulsion  $U-W$  and lead to charge transfer between the transition-metal (TM) sites.<sup>8</sup> In  $3d$  oxides this scenario is consistent with the observation of CD *only* for  $e_g^1$  orbitally degenerate systems close to the boundary between localized and itinerant behavior.

In this study we address the influence of the bandwidth  $W$  on the CD in the  $e_g^1 R\text{NiO}_3$  family. Larger  $W$ 's should reduce the JT distortions and favor the electron transfer between metallic sites but the opposite has been observed. The difference  $\Delta_d$  between the average Ni-O distance in the contracted  $\text{Ni}^{3+\delta}$  and expanded  $\text{Ni}^{3-\delta}$  sites, as determined by neutron powder diffraction, is significantly smaller for  $\text{PrNiO}_3$  (Ref. 6) than for  $\text{LuNiO}_3$ .<sup>1</sup> This suggests a smaller  $\delta$  in the former, despite its more delocalized nature. Larger values of  $\delta$  could be compatible with less pronounced structural changes if the transferred electrons are progressively delocalized out of the Ni-O bonds. Unfortunately, the lack of single crystals prevented to date the obtention of precise electronic density maps. Alternatively, the progressive emergence of dynamic charge/bond fluctuations in the insulating state has been proposed.<sup>6,9-11</sup>

## II. EXPERIMENT

Here we utilize a spectroscopic technique to get further insight in the evolution of  $\delta$  along the series.  $K$ -edge x-ray absorption spectroscopy in the partial fluorescence yield de-

tection mode (PFY-XAS) probes the valence configuration of the absorbing TM ion with enhanced sensitivity to fine spectral details over conventional XAS.<sup>12</sup> The energies of the  $4p$  absorption threshold, of the main edge (defined as the maximum of the first derivative), and of the pre-edge structures increase with the formal valence (Kunzl's law<sup>13</sup>). This dependence is approximately linear for absorbers with the same ligands and coordination polyhedra.<sup>14</sup> For oxides with octahedrally coordinated Ni, slopes of  $1-2$  eV/e<sup>-</sup> have been reported.<sup>15,16</sup>

Polycrystalline  $RNiO_3$  samples with  $R=La, Pr, Nd, Sm, Eu, Gd, Ho, Er, Tm, Yb,$  and  $Lu$  were prepared as described in Ref. 1. PFY-XAS measurements were performed at beamline ID26 at the European Synchrotron Radiation Facility (Grenoble, France), using radiation from two undulator sources monochromatized by Si(311) or Si(220) double-crystal monochromators. The beam scattered by the sample was analyzed by a Rowland circle spectrometer equipped with a spherically bent Si(620) crystal and detected by a photoavalanche diode. The intensity of the Ni  $K\alpha_1$  fluorescence ( $2p \rightarrow 1s$ ,  $h\nu_{out}=7478$  eV) was measured at room temperature (RT) for all samples while scanning the energy of the incident beam between 8330 and 8380 eV, across the Ni  $K$  absorption edge. The energy scale was calibrated at the beginning of the experiment using the maximum of the first derivative of a sheet of metallic Ni. The measurement was repeated several times during the experiment (typically every 3 h). The changes were always smaller than  $\pm 0.2$  eV. Low- and high-temperature PFY-XAS spectra were also recorded for selected samples ( $T=6$  K for La, Pr, and Nd, 573 K for Gd, and 623 K for Lu) using, respectively, a He cryostat and a furnace.

### III. DISCUSSION

The Ni  $K$  edges of metallic  $LaNiO_3$  (RT) and of the remaining samples in the insulating state are shown in Fig. 1(a). The raw spectra were divided by the incoming photon intensity and normalized at  $E=8368.3$  eV. PFY-XAS spectra of metallic Ni, NiO, and  $LaNiO_3$ , with formal valences 0, +2, and +3, are shown for comparison in Fig. 1(b). To be noted is the clear displacement of the edge toward lower energies for decreasing valences. By contrast, the  $RNiO_3$  spectra cross at a common energy corresponding to the maximum slope of the main edge, as expected from compounds with the same nominal valence. Figure 1(c) shows an enlarged view for the two end members of the family. Whereas the line shape of  $LaNiO_3$  is nearly structureless, that of  $LuNiO_3$  displays a steplike structure, clearly visible also in the pre-edge. This suggests that  $LuNiO_3$  Ni  $K$  edge is in fact a superposition of two similar line shapes shifted by  $\pm 1.5$  eV with respect to that of  $LaNiO_3$  (see ticks indicating the splitting of the maxima).

In order to check the existence of a similar splitting in the remaining members of the family, the first derivative was calculated for all spectra (see Fig. 2). For  $LaNiO_3$  we observe single, sharp maxima at 8333.5 and 8348.4 eV. All the other nickelates exhibit a double-peak structure at *both* the main edge (A and B features) and at the pre-edge (a and b

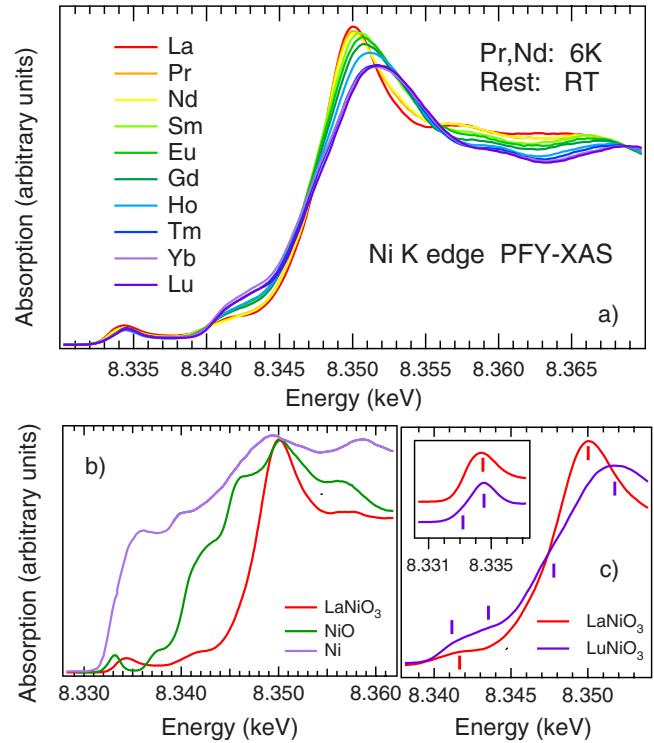


FIG. 1. (Color online) (a) Ni  $K\alpha$  PFY-XAS spectra of  $RNiO_3$  perovskites. La: metallic; Pr to Lu: insulating. (b) Ni  $K\alpha$  PFY-XAS spectra of metallic Ni, NiO, and  $LaNiO_3$ . (c) Detail of the main edge and the pre-edge (inset) for  $R=La$  and  $Lu$ .

features). The separation decreases for larger  $R$  ions but the splitting is clearly observable from  $R=Lu$  to  $Eu$ . It is less apparent for  $R=Sm, Nd,$  and  $Pr$  but a comparison (not

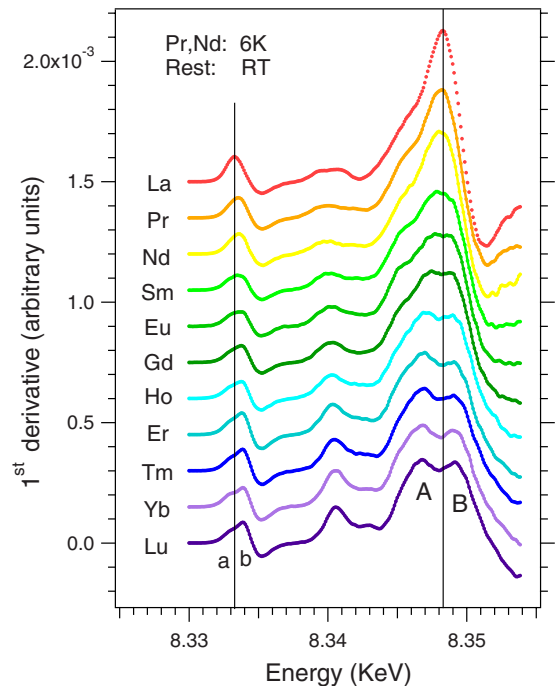


FIG. 2. (Color online) First derivative of the Ni  $K\alpha$  PFY-XAS spectra of  $RNiO_3$  perovskites.

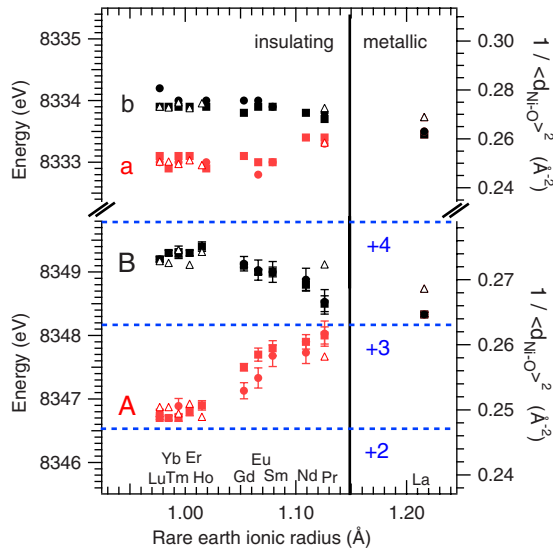


FIG. 3. (Color online) Left axis, full symbols: evolution of the position of the a, b, A, and B features along the  $RNiO_3$  series. Squares and circles correspond to two independent measurements performed at different times on different sample sets. Right axis, open symbols:  $1/d^2$ , where  $d$  is the average Ni-O distance in the  $Ni^{3+\delta}$  (black triangles along b/B) and  $Ni^{3-\delta}$  (red triangles along a/A) sites (Refs. 1 and 6). Blue dashed lines indicate the average edge positions reported for octahedrally coordinated Ni oxides with nominal valences +2, +3, and +4.

shown) between the first derivatives above and below  $T_{MI}$  for both Nd and Pr clearly indicates the presence of extra broadening in the low-temperature insulating state.

The energies of the A and B features were determined by fitting the line shapes of Fig. 2 with two Gaussians. The full width at half maximum was fitted independently for all samples with the exception of Sm, Nd, and Pr, where it was fixed to the values obtained for  $EuNiO_3$ . The resulting splitting  $\Delta_{AB}=(E_B-E_A)$  is five times larger for  $LuNiO_3$  [2.5(1) eV] than for  $PrNiO_3$  [0.5(3) eV]. For the a and b features the number of points was too small to obtain convergence and the maxima were determined manually. The results, displayed in Figs. 3(a) and 3(b), were fully reproducible (see caption) and confirm the progressive splitting of both the pre-edge and the main edge along the  $4f$  series.

The energies of both the a/b and A/B features scale as  $1/d^2$  ( $d$  is the average Ni-O distance) for the  $Ni^{3-\delta}/Ni^{3+\delta}$  sites, as already reported for absorbers with the same coordination polyhedra (see Ref. 17 and references therein). The nearly constant values of a, b, A, and B observed for the heavier nickelates ( $R=Lu$  to  $Ho$ ) and the faster evolution of a and A with the size of the lanthanide for  $R=Gd$  to  $La$ , compared to b and B, are also reproduced by the structural data (open symbols, right axis). This is a strong indication that the changes in the a/b and A/B features reflect the progressive splitting of the single Ni site of  $LaNiO_3$  in two distinct sites with, respectively, shorter/longer Ni-O distances.

For  $3d$  TM compounds, nominal valences cannot be directly interpreted in terms of the number  $n_d$  of  $3d$  electrons. In the cuprates, for instance, formally  $Cu^{2+}$  corresponds to

$n_d \sim 9.4$  rather than 9.<sup>18</sup> Nevertheless, the observed spectral changes give valuable insight in the evolution of the nominal valence of the contracted and expanded sites. We have compared the energies of the two sub-edges in the  $RNiO_3$  family with those of other Ni oxides with the same coordination and nominal valences between 0 and +4. Combining literature data<sup>15,16</sup> with our own measurements on the perovskites  $LaNi_{0.8}Al_{0.2}O_{2.16}$  (+0.9) and  $Sr_2NiWO_6$  (+2) we obtain a nearly linear relationship with a slope of about  $1.5 \text{ eV}/e^-$ . Application of this calibration curve to  $RNiO_3$  yields nominal valences very close to +4 and +2 for the  $Ni^{3+\delta}$  and  $Ni^{3-\delta}$  sites in the heavier  $R$ 's [see Fig. 3(b)], and very close to +3 for  $PrNiO_3$ . In other words, the two Ni  $K$  subedges observed in  $LuNiO_3$  are very close to those reported for single-valent compounds containing formally divalent/tetravalent Ni, whereas for  $PrNiO_3$  they nearly coincide with the value reported for nominally trivalent Ni. We thus conclude that, from the point of view of XAS and in contrast with previous predictions, the strength of the CD decreases by approaching the itinerant limit.

Although this finding qualitatively coincides with the conclusions of previous structural studies, XAS yields a larger difference between the nominal valences of the two end members of the series than that inferred from the interatomic distances.<sup>6</sup> A possible reason may be that neutrons are scattered by nuclei and probe electronic charges only indirectly, in particular, for materials close to the itinerant limit. The possible coexistence of the static CD with dynamic charge fluctuations faster than the interaction time of neutrons ( $\tau_n \sim 10^{-12} \text{ s}$ ) but slower than that of XAS ( $\tau_{XAS} \sim 10^{-14} \text{ s}$ ) could be at the origin of this difference. A further source of discrepancy could be the existence of a small, additional static distortion, not described by the low temperature  $P2_1/n$  symmetry but compatible with the anomalously large zero-point mean-square displacements reported for of the basal oxygens.<sup>6</sup> In particular, the existence of polar atomic displacements and the simultaneous existence of ferroelectricity below  $T_N \leq T_{MI}$  has been theoretically predicted.<sup>8,19</sup>

The phenomenological correlation between positive-energy shifts and decreasing valence<sup>13</sup> has a theoretical justification. XAS probes the ground-state unoccupied density of states (DoS) of the relevant symmetry, modified by the core hole and by final-state effects.<sup>20</sup> For the Ni  $K$  edge, the excited electron is promoted into the broad, empty Ni  $4p$  states, making final-state correlation effects negligible. Core effects are also expected to be small because the final  $4p$  states are delocalized and the core hole is efficiently screened by the  $3d$  electrons (nearly itinerant in  $RNiO_3$  perovskites). Changes in the Ni  $K$  edge for different Ni valences are thus expected to be mostly due to the modifications in the ground-state Ni  $4p$  unoccupied DoS for different  $3d$  occupancies. Figure 4 shows density-functional band-structure calculations of the Ni  $4p$  unoccupied DoS of  $LaNiO_3$ ,  $LuNiO_3$ ,  $NiO$ , and metallic Ni using the code DMOL3.<sup>21</sup> For the local-density approximation, the experimental RT crystallographic structures and the Perdew-Wang functional were used. The near-edge features were covered by the all-electron double numeric with polarization functions local-orbital variational



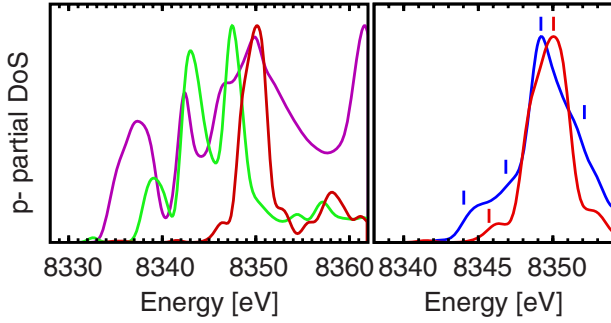


FIG. 4. (Color online) Left panel: DFT calculation of the Ni  $4p$  unoccupied DoS for  $\text{LaNiO}_3$  (red), NiO (green), and metallic Ni (purple). Right panel: comparison of the calculated Ni  $4p$  unoccupied DoS of  $\text{LaNiO}_3$  (red) and insulating  $\text{LuNiO}_3$  (blue). The color code is the same as in Figs. 1(b) and 1(c).

basis set. Brillouin-zone integration was done using the tetrahedron method with an  $8 \times 8 \times 8$  reciprocal space mesh for Ni metal and a  $2 \times 4 \times 2$  mesh for insulating  $\text{LuNiO}_3$ . As expected, explicit consideration of the core hole was found to have a negligible effect. To account for the (mainly relativistic) core-electron lowering plus the core-hole relaxation effects (assumed to be the identical for all compounds), all calculations were corrected by the same constant energy (215.2 eV), chosen to match the maximum of the  $\text{LaNiO}_3$  experimental spectrum with that of the calculated DoS. Although Lorentzian broadening due to the finite core-hole lifetime was not explicitly considered, a Gaussian broadening of 0.5 eV was applied in order to get a partial  $4p$  DoS slightly sharper than the experimental spectra.

In spite of discrepancies in the intensities, mostly due to the limited set of states displayed in the figure (only Ni  $4p$ ) and the nonconsideration of complex dynamical effects associated to the XAS process, the agreement between the DFT calculation and the XAS spectra is remarkable. For a given compound, the relative positions of the experimental features coincide well ( $\pm 1.5$  eV) with the maxima of the calculated Ni  $4p$  DoS. As shown in Fig. 4(b), the splitting in the Ni  $K\alpha$  edge of  $\text{LuNiO}_3$  with respect to  $\text{LaNiO}_3$  could be also reproduced. Even more noticeable is that the energy shifts of the NiO and metallic Ni  $K$  edges with respect to that of  $\text{LaNiO}_3$  are very close to the experimental values. This finding strongly supports a predominantly DoS origin for this effect and provides strong theoretical support to our phenomenological analysis.

We would like now to compare these results with those reported for charge-ordered manganese and iron perovskite oxides. As in the  $R\text{NiO}_3$  family, evidence for charge order (and in some cases for charge disproportionation) comes mostly from diffraction techniques. However, and in contrast to the results of this study, attempts to observe separate signatures of the two-ordered species using x-ray spectroscopies failed to date.<sup>22–25</sup> Since the chemical shifts reported in Mn and Fe oxides are significantly larger than in their Ni counterparts [ $\sim +4.2$  (Refs. 22 and 23) and  $\sim +2.5$  eV/ $e^-$ ,<sup>25</sup> respectively), this suggest that the formal valences of the two-ordered species in both ferrites and manganites are extremely close. For manganites, a possible reason for this different

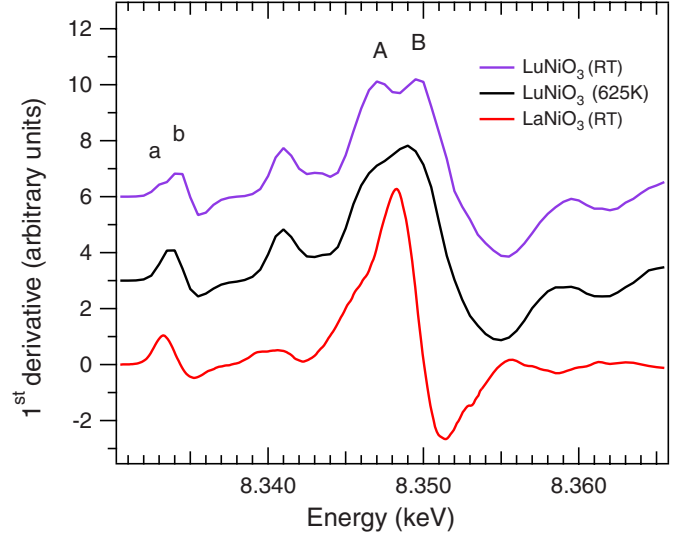


FIG. 5. (Color online) Ni  $K\alpha$  PFY-XAS spectra of  $\text{LuNiO}_3$  above and below  $T_{\text{MI}}$  compared with that of metallic  $\text{LaNiO}_3$ .

behavior may be their larger intrinsic disorder due to the coexistence of two different cations on the A sites compared to stoichiometric nickelates. The formation of a different type of charge order (Zener polarons<sup>26</sup>) compatible with the diffraction data has been suggested as well. Energy resolution may also be an issue, as suggested by the observation of two distinct Fe sites in ferrites by Mossbauer spectroscopy.<sup>27</sup>

Figure 5 shows further (first-derivative) data of  $\text{LuNiO}_3$  below and above  $T_{\text{MI}}$ . Surprisingly, the line shapes of metallic  $\text{LuNiO}_3$  and the (also metallic)  $\text{LaNiO}_3$  are different. The peak is sharp for  $\text{LaNiO}_3$  whereas for  $\text{LuNiO}_3$  it exhibits shoulders at the positions of the two structures present in the insulating state. This could imply the coexistence of the insulating and metallic phases above  $T_{\text{MI}}$ . However, such coexistence, common in first-order phase transitions, has been reported only in the insulating phase [ $T < T_{\text{MI}}$  (Ref. 28)]. We propose instead that a fluctuating CD persists above  $T_{\text{MI}}$ , by analogy with the static JT distortions in  $\text{LaMnO}_3$  which become dynamic above  $T_C = 750$  K. For  $\text{LaMnO}_3$  the existence of a vibronic state involving real charge transfers above  $T_C$  has been suggested by extended x-ray-absorption fine structure measurements which, in contrast with neutron diffraction, were able to evidence static JT distortions above  $T_C$ .<sup>29</sup> If, as is the case for mixed-valent systems, charge fluctuations occur in the nickelates on a time scale of  $10^{-13}$  s,<sup>30</sup> the single Ni site observed by neutron diffraction would indeed reflect a  $\text{Ni}^{3+\delta}/\text{Ni}^{3-\delta}$  average. This scenario naturally explains the observation of correlated anomalies in the resistivity, the infrared absorption and the muon-spin-rotation ( $\mu\text{SR}$ ) relaxation rate for  $\text{YNiO}_3$ .<sup>31</sup> Clearly observable in a temperature range of more than 100 K above  $T_{\text{MI}}$ , these anomalies have been interpreted in terms of an intermediate phase where charge fluctuations would precede the freezing of the electrons below  $T_{\text{MI}}$ .

#### IV. SUMMARY AND CONCLUSIONS

In summary, high-resolution PFY-XAS data reveal a

rare-earth-dependent splitting of the Ni *K* edges, and two inequivalent Ni sites in the insulating state for the whole RNiO<sub>3</sub> family. The evolution of the energy separation along the series suggests a much larger charge transfer for the heavier nickelates than previous studies. It also contradicts the predictions of a progressive increase in the charge transfer between TM sites by approaching the itinerant limit. The signatures of the Ni<sup>3+ $\delta$</sup>  and Ni<sup>3- $\delta$</sup>  sites are clearly observable 25 K above  $T_{MI}$  for  $R=Lu$ , suggesting that charge fluctuations persist well above  $T_{MI}$ . This unexpected result calls for

future XAS measurements covering an extended temperature range above  $T_{MI}$ .

#### ACKNOWLEDGMENTS

We are grateful to the ESRF for the allocation of beam time, as well as to the Swiss National Science Foundation, the National Center of Competence in Research MaNEP, and the Spanish Ministry of Education for financial support. Enlightening discussions with C. M. Varma, D. Khomskii, and Ch. Mudry are kindly acknowledged.

\*Present address: Laboratoire de Mathématiques, Physique et Systèmes, Université de Perpignan via Domitia, 52 Avenue de Paul Alduy, 66860 Perpignan Cedex, France

†Present address: Faculty of Physics and Applied Computer Science, AGH University of Science and Technology, Av. Mickiewicza 30, 30-059 Krakow, Poland

- <sup>1</sup>J. A. Alonso, M. J. Martínez-Lope, M. T. Casais, J. L. García-Munoz, and M. T. Fernández-Díaz, *Phys. Rev. B* **61**, 1756 (2000).
- <sup>2</sup>J. A. Alonso, J. L. García-Munoz, M. T. Fernández-Díaz, M. A. G. Aranda, M. J. Martínez-Lope, and M. T. Casais, *Phys. Rev. Lett.* **82**, 3871 (1999).
- <sup>3</sup>U. Staub, G. I. Meijer, F. Fauth, R. Allenspach, J. G. Bednorz, J. Karpinski, S. M. Kazakov, L. Paolasini, and F. d'Acapito, *Phys. Rev. Lett.* **88**, 126402 (2002).
- <sup>4</sup>M. Zaghrioui, A. Bulou, P. Lacorre, and P. Laffez, *Phys. Rev. B* **64**, 081102(R) (2001).
- <sup>5</sup>F. P. de la Cruz, C. Piamonteze, N. E. Massa, H. Salva, J. A. Alonso, M. J. Martínez-Lope, and M. T. Casais, *Phys. Rev. B* **66**, 153104 (2002).
- <sup>6</sup>M. Medarde, M. T. Fernández-Díaz, and P. Lacorre, *Phys. Rev. B* **78**, 212101 (2008).
- <sup>7</sup>C. M. Varma, *Phys. Rev. Lett.* **61**, 2713 (1988).
- <sup>8</sup>I. I. Mazin, D. I. Khomskii, R. Lengsdorf, J. A. Alonso, W. G. Marshall, R. M. Ibberson, A. Podlesnyak, M. J. Martínez-Lope, and M. M. Abd-Elmeguid, *Phys. Rev. Lett.* **98**, 176406 (2007).
- <sup>9</sup>M. Medarde, P. Lacorre, K. Conder, F. Fauth, and A. Furrer, *Phys. Rev. Lett.* **80**, 2397 (1998).
- <sup>10</sup>P. Ruello, S. Zhang, P. Laffez, B. Perrin, and V. Gusev, *Phys. Rev. B* **76**, 165107 (2007).
- <sup>11</sup>J.-S. Zhou, J. B. Goodenough, and B. Dabrowski, *Phys. Rev. B* **67**, 020404(R) (2003).
- <sup>12</sup>K. Hamalainen, D. P. Siddons, J. B. Hastings, and L. E. Berman, *Phys. Rev. Lett.* **67**, 2850 (1991).
- <sup>13</sup>V. Kunzl, *Collect. Trav. Chim. Tchécoslovaquie* **4**, 213 (1932).
- <sup>14</sup>J. Wong, F. W. Lytle, R. P. Messmer, and D. H. Maylotte, *Phys. Rev. B* **30**, 5596 (1984).
- <sup>15</sup>M. Crespín, P. Levitz, and L. Gatineau, *J. Chem. Soc., Faraday Trans.* **79**, 1181 (1983).
- <sup>16</sup>A. N. Mansour and C. Melendres, *J. Phys. Chem. A* **102**, 65 (1998).
- <sup>17</sup>H. Tolentino, M. Medarde, A. Fontaine, F. Baudelet, E. Dartyge, D. Guay, and G. Tourillon, *Phys. Rev. B* **45**, 8091 (1992).
- <sup>18</sup>H. Eskes, L. H. Tjeng, and G. A. Sawatzky, *Phys. Rev. B* **41**, 288 (1990).
- <sup>19</sup>G. Giovannetti, S. Kumar, D. Khomskii, S. Picozzi, and J. van den Brink, *Phys. Rev. Lett.* **103**, 156401 (2009).
- <sup>20</sup>M. Grioni, J. F. van Acker, M. T. Czyzyk, and J. C. Fuggle, *Phys. Rev. B* **45**, 3309 (1992).
- <sup>21</sup>B. Delley, *J. Chem. Phys.* **113**, 7756 (2000).
- <sup>22</sup>G. Subías, J. García, M. G. Proietti, and J. Blasco, *Phys. Rev. B* **56**, 8183 (1997).
- <sup>23</sup>M. Croft, D. Sills, M. Greenblatt, C. Lee, S.-W. Cheong, K. V. Ramanujachary, and D. Tran, *Phys. Rev. B* **55**, 8726 (1997).
- <sup>24</sup>J. García, M. Sánchez, G. Subías, and J. Blasco, *J. Phys.: Condens. Matter* **13**, 3229 (2001).
- <sup>25</sup>J. Blasco, B. Aznar, J. García, G. Subías, J. Herrero-Martin, and J. Stankiewicz, *Phys. Rev. B* **77**, 054107 (2008).
- <sup>26</sup>A. Daoud-Aladine, J. Rodríguez-Carvajal, L. Pinsard-Gaudart, M. T. Fernández-Díaz, and A. Revcolevschi, *Phys. Rev. Lett.* **89**, 097205 (2002).
- <sup>27</sup>M. Takano, J. Kawachi, N. Nakanishi, and Y. Takeda, *J. Solid State Chem.* **39**, 75 (1981).
- <sup>28</sup>X. Granados, J. Fontcuberta, X. Obradors, and J. B. Torrance, *Phys. Rev. B* **46**, 15683 (1992).
- <sup>29</sup>M. C. Sánchez, G. Subías, J. García, and J. Blasco, *Phys. Rev. Lett.* **90**, 045503 (2003).
- <sup>30</sup>I. Nowik, *Hyperfine Interact.* **13**, 89 (1983).
- <sup>31</sup>J. L. García-Muñoz, R. Mortimer, A. LLobet, J. Alonso, M. Martínez-Lope, and S. Cottrell, *Physica B (Amsterdam)* **374-375**, 87 (2006).